



**HAL**  
open science

# A temperature- and photoperiod-driven model reveals complex temporal population dynamics of the invasive box tree moth in Europe

Christelle Suppo, Audrey Bras, Christelle Robinet

## ► To cite this version:

Christelle Suppo, Audrey Bras, Christelle Robinet. A temperature- and photoperiod-driven model reveals complex temporal population dynamics of the invasive box tree moth in Europe. *Ecological Modelling*, 2020, 432, pp.109229. 10.1016/j.ecolmodel.2020.109229 . hal-03123286

**HAL Id: hal-03123286**

**<https://hal.science/hal-03123286>**

Submitted on 27 Jan 2021

**HAL** is a multi-disciplinary open access archive for the deposit and dissemination of scientific research documents, whether they are published or not. The documents may come from teaching and research institutions in France or abroad, or from public or private research centers.

L'archive ouverte pluridisciplinaire **HAL**, est destinée au dépôt et à la diffusion de documents scientifiques de niveau recherche, publiés ou non, émanant des établissements d'enseignement et de recherche français ou étrangers, des laboratoires publics ou privés.

1 A temperature- and photoperiod-driven model reveals complex temporal  
2 population dynamics of the invasive box tree moth in Europe

3  
4  
5  
6  
7  
8  
9  
10 4 Christelle Suppo<sup>a</sup>, Audrey Bras<sup>b,c</sup> and Christelle Robinet<sup>b</sup>

11  
12 5 <sup>a</sup>Institut de Recherche sur la Biologie de l’Insecte, UMR 7261, CNRS –Université de Tours, F-37200  
13 6 Tours, France

14 7 <sup>b</sup>INRAE, URZF, F-45075 Orléans, France

15 8 <sup>c</sup>Unit of Chemical Ecology, Department of Plant Protection Biology, Swedish University of Agricultural  
16 9 Sciences, Alnarp, Sweden

17 10  
18 11  
19 12  
20 13 \* Corresponding author: [christelle.suppo@univ-tours.fr](mailto:christelle.suppo@univ-tours.fr)  
21 14  
22 15  
23 16  
24 17  
25 18  
26 19  
27 20  
28 21  
29 22  
30 23  
31 24  
32 25  
33 26  
34 27  
35 28  
36 29  
37 30  
38 31  
39 32  
40 33  
41 34  
42 35  
43 36  
44 37  
45 38  
46 39  
47 40  
48 41  
49 42  
50 43  
51 44  
52 45  
53 46  
54 47  
55 48  
56 49  
57 50  
58 51  
59 52  
60 53  
61 54  
62 55  
63 56  
64 57  
65 58

50 24 Number of tables: 5

51 25 Number of figures: 6

52 26  
53 27 **Journal: Ecological Modelling, species issue “ISEM 2019”**

54 28 **Type of paper: Original research paper**

29 **Abstract**

1  
2  
3 30 The box tree moth, *Cydalima perspectalis*, is an invasive insect that has rapidly colonised Europe,  
4  
5 31 damaging to natural and ornamental box trees. In its native habitat in China, the number of  
6  
7 32 generations per year is variable, but the number of generations observed in European climates  
8  
9 33 remained unclear. This is a key issue for understanding the rapid increase in population size and  
10  
11 34 range, and for optimising control. We developed a temperature- and photoperiod-driven model to  
12  
13 35 simulate the life cycle of this insect and development rates for each life stage. The model was  
14  
15 36 calibrated on published data and validated with observations obtained in France and Switzerland.  
16  
17 37 Model stability analysis showed that minimal temperature for larval development to be the most  
18  
19 38 important parameter to estimate. Diapause parameters had little effect. We then explored the  
20  
21 39 effects of temperature increases of 1 and 2°C. The number of generations ranged from two to four at  
22  
23 40 the various study sites. Climate warming will accelerate the insect life cycle, making it possible for the  
24  
25 41 occurrence of one more generation per year. The key finding of this study was the complexity of  
26  
27 42 population dynamics for this species. Some generations overlapped, making it difficult to identify the  
28  
29 43 adult flight period clearly for each generation. Furthermore, various stages were potentially able to  
30  
31 44 overwinter, not just diapausing larvae. Climate warming may also enhance this phenomenon in the  
32  
33 45 future. Further explorations of the complex dynamics of this species are required, notably it remains  
34  
35 46 unclear how successfully the various life stages survive winter temperatures. Further model  
36  
37 47 refinements are also required to obtain more accurate estimates of box tree moth phenology.  
38  
39 48 However, this is the first phenology model for box tree moth to be published, and our findings  
40  
41 49 provide useful information for improving control of this pest.  
42  
43  
44  
45  
46  
47  
48  
49  
50

51 50

54 51 **Keywords:** climate change; *Cydalima perspectalis*; phenology; diapause; modelling

57 52

53 **1. Introduction**

1  
2  
3 54 The number of biological invasions worldwide has steadily increased since 1800, but has not yet  
4  
5 55 reached saturation point (Seebens et al. 2017). The number of exotic arthropod invasions, in  
6  
7 56 particular, has increased spectacularly since the 16<sup>th</sup> century, with a clear acceleration in the second  
8  
9 57 half of the 20<sup>th</sup> century (Roques 2010). This increase in the number of invasions is partly attributable  
10  
11  
12 58 to the introduction of phytophagous species with the intensification of the international ornamental  
13  
14  
15 59 plant trade (Dehnen-Schmutz et al. 2010; Roques 2010).

16  
17  
18 60 Increases in the number of entries and the spread of exotic species within a new territory account for  
19  
20 61 the surge in biological invasions. Following their arrival in new territories, exotic insect species spread  
21  
22 62 at various rates, depending on the time since their introduction and their feeding guild. For example,  
23  
24  
25 63 species discovered since the 1990s tend to spread three to four times more rapidly than those  
26  
27 64 arriving before this time point (Roques et al. 2016). Exceptionally high dispersal capabilities generally  
28  
29  
30 65 drive this rapid range expansion. Some species can naturally disperse over very long distances (e.g.,  
31  
32 66 the invasive yellow-legged hornet; Robinet et al. 2017), can rapidly evolve the capacity for fast  
33  
34 67 dispersal (e.g., the bean beetle; Ochocki & Miller 2017), or may be transported over long distances by  
35  
36  
37 68 human activities, thanks to the free circulation of goods within the European Union, for example  
38  
39 69 (Roques et al. 2016). However, high dispersal capabilities alone cannot account for the rapid spread  
40  
41  
42 70 observed. Population growth is another key factor to be taken into account, as it might explain how  
43  
44 71 possible Allee effects are overcome at low population density (Taylor & Hastings 2005). Together  
45  
46 72 with dispersal capacity and population carrying capacity, population growth could drive the rate at  
47  
48  
49 73 which the invasion wave spreads (Shigesada & Kawasaki 1997; Haond et al. 2018). Thus, insects that  
50  
51 74 produce several generations per year are likely to spread more rapidly (Fahrner & Aukema 2018).

52  
53  
54 75 Population phenology modelling can be used to estimate the number of generations and the time  
55  
56 76 window associated with each life stage. The phenology model classically used to describe the  
57  
58  
59 77 development of plants and poikilothermic organisms, such as insects, is the degree-day model. This

1  
2  
3  
4  
5  
6  
7  
8  
9  
10  
11  
12  
13  
14  
15  
16  
17  
18  
19  
20  
21  
22  
23  
24  
25  
26  
27  
28  
29  
30  
78 model has proved accurate for many species over the years (Bonhomme 2000, Damos & Savopoulou-  
79 Soultani 2012, Rebaudo & Rabhi 2018). It is based on the principle that a number of thermal units  
80 above a given temperature threshold must be accumulated to complete the development of a given  
81 life stage, leading to definition of the heat accumulation required for development. In this model, we  
82 assume a linear relationship between temperature and development rate. Non-linear models have  
83 been developed to refine this modelling framework and to provide more subtle performance curves  
84 than linear relationships (Rebaudo & Rabhi 2018). However, these models require data for the fitting  
85 of these non-linear functions (e.g., experimental data for development rates as a function of  
86 temperature), which is feasible for only a set of well-documented species. These models, based on  
87 temperature-driven processes, can also be improved by considering: 1) photoperiod thresholds,  
88 particularly for organisms that have a dormancy or diapause period (Pollard et al. 2020) and 2)  
89 population growth (fecundity and mortality factors) (e.g., the agent-based model developed for the  
90 invasive brown marmorated stink bug, *Halyomorpha halys*, model, Nielsen et al. 2016).

31  
32  
33  
34  
35  
36  
37  
38  
39  
40  
41  
42  
43  
44  
45  
46  
47  
48  
49  
50  
91 A good knowledge of the biology of the species concerned is required for the parameterisation of  
92 such models and for the development of effective control measures limiting the spread of invasive  
93 species. However, the biology of invasive species is generally poorly understood, as most of these  
94 species cause no significant damage in their native area and some are even unknown to science  
95 (Seebens et al. 2017). In addition, the build-up of the population in the invaded area is subject to  
96 founder effects and genetic bottlenecks (Dlugosch & Parker 2008), and may not, therefore, be  
97 entirely representative of the characteristics of individuals in their native area. Careful study of the  
98 invasive population is, therefore, required, to assess its potential growth and spread.

51  
52  
53  
54  
55  
56  
57  
58  
59  
60  
61  
62  
63  
64  
65  
99 The box tree moth, *Cydalima perspectalis* (Walker, 1859) (Lepidoptera: Crambidae), is emblematic of  
100 a rapid invasion (Roques et al. 2016). It is native to Asia and it develops on box trees. It was first  
101 detected in Europe in Germany in 2007, and has since invaded a large area extending from France to  
102 Iran (Bras et al. 2019) and causing significant damage to European *Buxus* trees. It has a rate of spread

103 in Europe of up to 155 km/year. This rapid spread probably reflects multiple introductions from China  
104 on imported box trees (Bras et al. 2019), in addition to other factors, such as human-mediated  
105 dispersal through the box tree trade within the European Union (Bras 2018), and its own potential  
106 for population growth. The box tree moth has three to five generations per year in China (Wan et al.  
107 2014) but only two generations per year have been recorded in Switzerland (Nacambo et al. 2014). It  
108 remains unclear how many generations this moth could potentially produce in the various climates  
109 found in Europe. This species overwinters at the larval stage: from the 2<sup>nd</sup> to the 5<sup>th</sup> larval instar in  
110 China, depending on the precise geographic area (Wan et al. 2014), and mostly at the 3<sup>rd</sup>-4<sup>th</sup> larval  
111 instar stages in Europe (Nacambo et al. 2014; Bras 2018). The conditions required for diapause  
112 induction are relatively well known (day length of 13:30 hours in Europe; Nacambo et al. 2014 and  
113 day length of between 12:50 and 13:36 hours in China; Xiao et al. 2011), but those for the end of  
114 diapause remain unclear, making it difficult to predict when insects will resume their development in  
115 the spring.

116 In this study, we aimed to develop a temperature- and photoperiod-driven model (based mostly on a  
117 phenology model) to explore box tree moth phenology in detail and to determine how many  
118 generations this species can produce in Europe. The results of this study will ultimately improve our  
119 understanding of the spatiotemporal dynamics of this invasive species, and will also facilitate the  
120 temporal optimisation of pest management methods targeting particular stages in the life cycle.

## 2. Materials and Methods

### *2.1 Biology of the study species in its invaded range*

124 The box tree moth is a multivoltine species (Fig. 1).

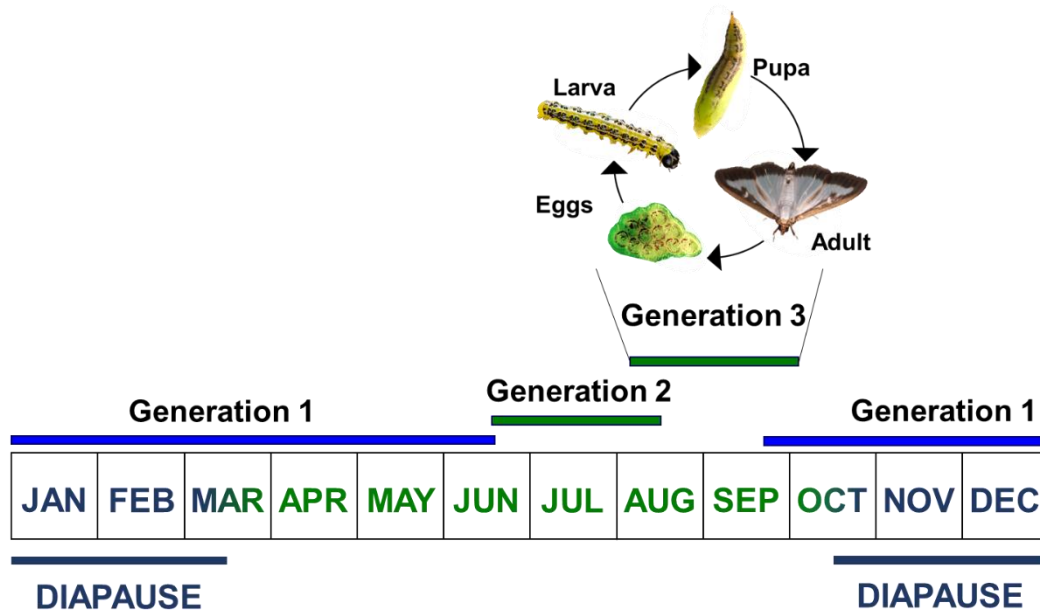
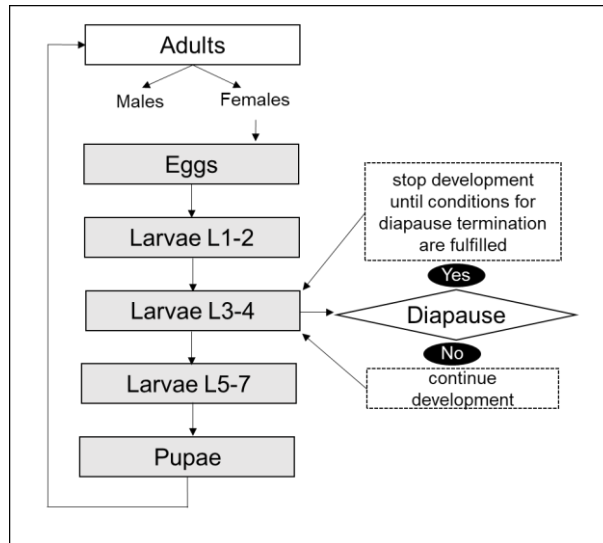


Fig. 1. Box tree moth life cycle and timeline for three generations per year, as is thought to occur in some parts of Europe. The life cycle is illustrated for Generation 3. The period of the year during which the moth is active is shown in green and the overwintering period is shown in blue. The first generation (Generation 1) is the overwintering generation.

Throughout most of the invaded range, this insect is active from late March to late October. Two to three generations per year have been recorded in several parts of Europe (Nacambo et al. 2014; Matošević et al. 2017), but it is thought that up to four generations per year may occur in Georgia (Gninenko et al. 2014). The moth overwinters at the larval stage, in cocoons stuck to the leaves of box trees. The overwintering cocoons can be observed from September (when day length falls below about 13 h) until the spring. The factors involved in diapause termination remain unclear, but exposure to cold temperatures for at least one and a half months may be required for the insect to resume its development (Nacambo et al. 2014). The overwintering larvae usually complete their development in spring, when temperatures start to increase. The first adults are observed in June and the second and third generations are produced during the summer.

142 **2.2. Description of the phenology model**

143 For each life stage, from eggs to pupae, we consider a degree-day model (Fig. 2).



144  
145 Fig. 2. Diagram of the *Cydalima perspectalis* life stage model. Grey rectangles indicate life stages for  
146 which a degree-day model is applied.

148 We considered the accumulation of temperature above a given lower developmental threshold ( $TL$ )  
149 and below a given upper developmental threshold ( $TU$ ), and assumed that the development of the  
150 stage was complete when the number of degree-days required for the stage development ( $DD$ ) was  
151 reached. We used the double-sine wave method to calculate the number of degree-days  
152 accumulated (Zalom et al. 1983). In this method, temperatures are interpolated from the daily  
153 minimal and maximal temperatures, by half-days, with a sinusoidal curve and the area under the  
154 curve between  $TL$  and  $TU$  is calculated. For larvae, we did not consider each of the individual larval  
155 stages (from L1 to L7), because too few data were available to parameterise the model. Instead, we  
156 considered three groups of larval stages: G1 corresponding to L1-L2, G2 corresponding to L3-L4, and  
157 G3 corresponding to L4-L7, because only G2 is likely to enter diapause for winter and, therefore, to  
158 experience an interruption of larval development.

159 The dates of diapause induction and termination were calculated from the photoperiod and  
1 temperature datasets (daily minimal and maximal temperatures). Diapause can begin when  
2 160 temperature datasets (daily minimal and maximal temperatures). Diapause can begin when  
3  
4 161 photoperiod falls below a day length of  $DI$ . For any day after this date and before November (after  
5  
6  
7 162 November, we considered the temperature to be too low), cold was accumulated and we  
8  
9 163 determined the date by which sufficient exposure to cold had been accumulated ( $DL_{cold}$  days at  
10  
11 164 which the minimal temperature was below  $TL_{cold}$ ). After this date, heat began to accumulate, and  
12  
13  
14 165 we calculated the date at which sufficient heat accumulation had been achieved ( $DU_{warm}$   
15  
16 166 consecutive days during which the maximal temperature was above  $TU_{warm}$ ). Once sufficient heat  
17  
18  
19 167 has been accumulated, overwintering ends and the larvae can continue their development. We also  
20  
21 168 calculated a mortality rate for the diapause period, based on cold accumulation (see model  
22  
23 169 parameterisation).

26 170 The model was initiated with a flight curve providing the number of individuals flying each day, to  
27  
28  
29 171 represent the number of adults emerging each day. We assumed that the males and females  
30  
31 172 emerged at the same time (Göttig 2017) and that the sex ratio was 0.5 (Tabone et al. 2015, Göttig  
32  
33  
34 173 2017). We then needed to know the number of fertilised females to calculate the number of eggs.  
35  
36 174 Assuming that males and females are randomly distributed in space, the probability of mating  
37  
38 175 success follows a Poisson probability distribution (Boukal & Berec 2002). The number of fertilised  
39  
40  
41 176 females is therefore:  $N_f \times (1 - \exp(-N_m))$ , where  $N_f$  and  $N_m$  are the number of adult females  
42  
43 177 emerging on a given day and the number of adult males present on that day, respectively (Robinet et  
44  
45  
46 178 al. 2007). This quantity rapidly tends toward  $N_f$  as  $N_m$  increases, and is therefore weakly constrained  
47  
48 179 by the number of males. We simulated egg-laying according to this flight curve, by distributing the  
49  
50  
51 180 number of eggs laid by each female ( $FEC$ ) over a period of time after emergence ( $DayEgg$ ). We then  
52  
53 181 applied the degree-day model for eggs (with  $TL=TL_{eggs}$  and  $DD=DD_{eggs}$ ), for larva groups G1, G2 and  
54  
55 182 G3 (with  $TL=TL_{larvae1}$ ,  $TL_{larvae2}$ ,  $TL_{larvae3}$ , and  $DD=DD_{larvae1}$ ,  $DD_{larvae2}$ ,  $DD_{larvae3}$ ,  
56  
57  
58 183 respectively), and for pupae (with  $TL=TL_{pupae}$  and  $DD=DD_{pupae}$ ). For each stage, we applied a  
59  
60 184 mortality rate ( $m_{eggs}$ ,  $m_{larvae1}$ ,  $m_{larvae2}$ ,  $m_{larvae3}$ ,  $m_{pupae}$ ,  $m_{adult}$ ) before simulating the

185 development of the next stage. Once pupae complete their development, the adults emerge and are  
 186 assumed to live for a certain period (*longevity*). The females then lay eggs and the algorithm moves  
 187 on to the next loop (Fig. 2).

188 In addition, for G2 (L3-L4), we also tested whether the date (considered incrementally, day after day)  
 189 could be considered a date on which they could enter diapause, for each day of their development.  
 190 Larvae entering diapause were considered to stop developing, with development beginning again  
 191 after the end of diapause.

192 In total, 24 input parameters must be provided to simulate the phenology of the box tree moth  
 193 (Table 1). The model was coded in R language (R Core Team 2019; Robinet & Suppo 2020).

Parameter	Default value	Description
<i>NF</i>	1000	Number of female adults at time $t=0$
<i>DI</i>	13 h	Photoperiod triggering winter diapause
<i>TLcold</i>	2°C	Temperature threshold below which cold is accumulated for diapause
<i>DLcold</i>	45 days	Number of days during which minimal temperature should be below <i>TLcold</i> to accumulate cold for diapause
<i>TUwarm</i>	vector(5,10,15,20)	Maximal temperature thresholds (°C) for determining the end of diapause
<i>DUwarm</i>	vector(28,9,7,3)	Number of consecutive days during which maximal temperature should be above <i>TUwarm</i> to achieve diapause. As soon as a condition is fulfilled (e.g., the second condition, daily maximal temperature is >10°C during 9 consecutive days), we considered the heat required to complete diapause to have accumulated.
<i>F</i>	2	Number of eggs laid by each female
<i>Deggs</i>	Day 4 to 14 after adult emergence (spread over 11 days)	Days after adult emergence on which eggs are laid by females
<i>L</i>	14 days	Adult longevity
<i>TLeggs</i>	10.91°C	Temperature threshold above which degree-days are accumulated for eggs
<i>DDeggs</i>	48.54°C days	Sum of degrees above <i>TLeggs</i> necessary for egg development
<i>TLlarvae</i>	8.38°C	Temperature threshold above which degree-days are accumulated for larvae
<i>DDLarvae1</i>	44.5°C days	Sum of degrees above <i>TLlarvae</i> necessary for the development of larvae (L1-2)
<i>DDLarvae2</i>	66.7°C days	Sum of degrees above <i>TLlarvae</i> necessary

		for the development of larvae (L3-4)
<i>DDLarvae3</i>	211.3°C days	Sum of degrees above <i>TLlarvae</i> necessary for the development of larvae (L5-7)
<i>TLpupae</i>	11.5°C	Temperature threshold above which degree-days are accumulated for pupae
<i>DDpupae</i>	133.33°C days	Sum of degrees above <i>TLpupae</i> necessary for pupae development
<i>meggs</i>	0.1	Mortality rate of eggs
<i>mlarvae1</i>	0.2	Mortality rate of larvae L1-2 (G1)
<i>mlarvae2</i>	0.05	Mortality rate of larvae L3-4 (G2)
<i>mlarvae3</i>	0.05	Mortality rate of larvae L5-7 (G3)
<i>mpupae</i>	0.02	Mortality rate of pupae
<i>madults</i>	0.05	Mortality rate of adults
<i>fmort</i>	<i>function</i>	Mortality (as a %) for diapausing larvae (derived from Nacambo et al. 2014)

**Table 1.** List of model parameters.

### 2.3. Model parameterisation

*Development thresholds.* The estimates of *TL* and *DD* for each stage were mostly obtained from the work of Nacambo et al. (2014), who studied an invasive population in Switzerland (Europe). We thus considered *TLeggs* = 10.91°C and *DDeggs* = 48.54 degree-days, and *TLpupae* = 11.5°C and *DDpupae* = 133.33 degree-days. For larval stage, Nacambo et al. (2014) showed that the lower temperature threshold was 8.38°C and that 322.58 degree-days were required for development. Since we considered three groups of larval stages (L1-2, L3-4 and L5-7), we assumed that *TLlarvae1* = *TLlarvae2* = *TLlarvae3* = 8.38°C. In a study conducted in Asia, Maruyama & Shinkaji (1991) found that stages L1 to L5 each completed development within three days, and that stage L6 completed development within eight days at 25°C. Since we have observed that L1 individuals originating from the invasive population develop much more rapidly than L2-L5 larvae, we considered only one day of development to be required for L1. We also assumed that L7 larvae developed at the same rate as L6 larvae (i.e. within 8 days). Thus, at 25°C, the total duration of larval development from L1 to L7 would be 29 days. According to Tabone et al. (2015), the duration of the larval stage is between 29 and 33

211 days for a population sampled within the invaded range in Europe. The two estimates are, thus,  
212 consistent. We then derived the number of degree-days above 8.38°C required from the number of  
213 days of development at 25°C, and we found that:  $DD_{larvae1} = 44.5$  degree-days,  $DD_{larvae2} = 66.7$   
214 degree-days, and  $DD_{larvae3} = 211.3$  degree-days. As no information was available about the upper  
215 developmental threshold, we assumed that  $TU_{eggs} = TU_{larvae1} = TU_{larvae2} = TU_{larvae3} = TU_{pupae}$   
216 = + infinity. This is a conservative assumption for the sites considered here, since individuals can  
217 probably develop at temperatures of up to 35°C (Nacambo et al. 2014), and the model was applied to  
218 regions in which maximal temperatures in summer are generally around this threshold. More  
219 rigorous testing of the effects of heatwaves, during which temperatures may reach 40°C, would  
220 require improvements in the assessment of this parameter. In this study, we focus on average  
221 temperatures, ignoring extreme climate events.

222 *Diapause conditions.* Photoperiod is an important factor for diapause induction. Taking into account  
223 the work of Nacambo et al. (2014) and Xiao et al. (2010), we assumed that diapause was induced as  
224 soon as the photoperiod fell below 13 h of daylight ( $DI = 13$  h). The conditions for the end of  
225 diapause still remained uncertain. Diapausing larvae must first accumulate a certain amount of cold.  
226 In accordance with the findings of Nacambo et al. (2014), we considered that minimal temperatures  
227 had to be below  $TL_{cold} = 2^{\circ}\text{C}$  for a period  $DL_{cold} = 45$  days. After accumulating cold, the larvae have  
228 to accumulate heat to end diapause. Based on the results of laboratory experiments on L4 under a  
229 photoperiod of 10-12 hours (Bras 2018; Poitou 2018), we assumed that a maximal temperature of at  
230 least 5, 10, 15, or 20°C ( $TU_{warm}$ ) for 28, 9, 7 or 3 consecutive days ( $DU_{warm}$ ), respectively, was  
231 required. The larvae can continue their development if one of these conditions is fulfilled.

232 *Mortality rates.* Except for eggs, no data were available for the accurate estimation of mortality at  
233 each stage. Based on observations and extrapolations from field data, we considered:  $meggs = 10\%$   
234 (Lepilleur et al. 2017),  $mlarvae1 = 20\%$ ,  $mlarvae2 = 5\%$ ,  $mlarvae3 = 5\%$ ,  $mpupae = 2\%$ ,  $madult = 5\%$   
235 (Elisabeth Tabone, Pers. Com.). These estimates are subject to a high degree of uncertainty, but this

236 uncertainty affects the population level rather than the time window for each stage and generation.

237 In addition to these mortality rates, we considered mortality during the winter diapause. Nacambo et  
238 al. (2014) showed that mortality rate during diapause depends on the duration for which larvae were  
239 exposed to a temperature of 2°C or lower during the overwintering period. We used the following  
240 function to estimate this mortality rate (in %), which ranged from 90% when cold accumulation was  
241 very short (<1 month) to 10% when it lasted 3.5 months:

$$f_{mort}(x) = \begin{cases} 90 & \text{if } x < 30\text{days} \\ 100 - (2.67(x - 45) + 50) & \text{if } 30 \leq x < 45\text{days} \\ 100 - (0.67(x - 60) + 60) & \text{if } 45 \leq x < 60\text{days} \\ 100 - (0.67(x - 75) + 70) & \text{if } 60 \leq x < 75\text{days} \\ 100 - (0.67(x - 90) + 80) & \text{if } 75 \leq x < 90\text{days} \\ 100 - (0.67(x - 105) + 90) & \text{if } 90 \leq x < 105\text{days} \\ 100 - (-0.67(x - 120) + 80) & \text{if } 105 \leq x < 120\text{days} \\ 100 + 1.33(x - 180) & \text{if } x \geq 120\text{days} \end{cases}$$

242 with  $x$  the number of days at which the daily minimal temperature was below 2°C during the  
243 diapause period.

244 *Other biological parameters.* According to Tabone et al. (2015), female adults can live for 12 days and  
245 male adults can live for 15 days under laboratory conditions (25°C). We therefore assumed that  
246 adults of both sexes could live for  $L = 14$  days in the field. Each female lays a mean of 800 eggs ( $\pm 300$   
247 eggs) (Tabone et al. 2015). As we aimed to study the phenology of the insects rather than their  
248 abundance, we used a fecundity  $F = 2$  in subsequent simulations, to avoid a surge in the size of the  
249 population and problems visualising the number of individuals. We also needed to enter the number  
250 of females initially present,  $NF$ , to initiate the model. We chose an arbitrary value for this,  $NF = 1000$ .

251

## 252 **2.4. Model validation**

253 The model was validated in four ways: a preliminary check and three validations on independent  
254 datasets: 1) for four sites at which adult flights were recorded with pheromone traps in two

255 consecutive years, 2) for one site at which adult flights were recorded in four consecutive years and  
1  
2 256 3) for one site at which all life stages were followed for a whole year (Pineau et al. 2020).  
3  
4 257 Preliminary check. We compared the predicted phenology (duration of each life stage) at a constant  
5  
6 258 temperature of 25°C with the laboratory observations reported by Tabone et al. (2015).  
7  
8  
9 259 Validation 1. We compared the predicted time-window of adult occurrence, according to simulations,  
10  
11 260 with trap captures at several locations. We considered trap captures in 2017 and 2018 at Orléans  
12  
13 261 (47.83°N, 1.91°E, 105 m asl), Contrevoz (45.80°N, 5.63°E, 370 m asl), and Caen (49.18°N, -0.37°W, 10  
14  
15 262 m asl) in France. We also considered the data of Nacambo et al. (2014) for Basel and Riehen  
16  
17 263 (Switzerland) in 2011 and 2012. Basel and Riehen are only 5 km apart. We therefore considered them  
18  
19 264 to constitute a single site, referred to hereafter simply as “Basel”. We initiated the model on the first  
20  
21 265 flight of the first year and validation was performed in the second year. We calculated the  
22  
23 266 correctness rate of presences and absences, between observations and simulation results.  
24  
25 267 Temperature data were retrieved from the nearest weather station, at Orléans, Belley (about 6 km  
26  
27 268 from Contrevoz), Caen, and Basel. The temperature data for French sites were provided by Météo-  
28  
29 269 France and those for the Swiss site were retrieved from <http://www.ecad.eu> (Klein Tank et al. 2002).  
30  
31 270 Photoperiod data were retrieved from <http://www.soda-pro.com> (SoDa team 2019).  
32  
33 271 Validation 2. We explored the cumulative error of the model over the years, using the data from  
34  
35 272 Nacambo et al. (2014) for Basel in 2009 (first flight) to initiate the model, and simulating insect  
36  
37 273 phenology until 2012. We calculated the correctness rate of presences and absences, between  
38  
39 274 observations and simulation results for 2010, 2011 and 2012.  
40  
41 275 Validation 3. Finally, we validated the model with a more comprehensive dataset (from eggs to  
42  
43 276 adults) collected in Orléans from 2018 to 2019 (Pineau et al. 2020). Trap captures were checked over  
44  
45 277 a longer period (i.e., from April 28<sup>th</sup> to November 6<sup>th</sup> 2018, and from April 24<sup>th</sup> 2019 to November  
46  
47 278 29<sup>th</sup> 2019), to ensure that both the earliest and latest flights were recorded. Two pheromone traps  
48  
49 279 were frequently checked (two to seven times per week, following the flight season). At the INRAE  
50  
51 280 nursery in Orléans, 30 box trees (1.50 m high) were checked for three minutes each. The numbers of  
52  
53  
54  
55  
56  
57  
58  
59  
60  
61  
62  
63  
64  
65

281 eggs, small larvae (G1: L1-L2), medium-sized larvae (G2: L3-L4), large larvae (G3: L5-L7), pupae and  
282 diapausing larvae were counted. Life cycle stages were observed weekly from June 21<sup>st</sup> 2018 to  
283 October 31<sup>st</sup> 2018, monthly during the cold season (from November 2018 to May 2019) and then  
284 weekly again until June 21<sup>st</sup> 2019. The larvae found in the dense silk cocoons on the box tree leaves  
285 were assumed to be diapausing larvae. To our knowledge, this dataset, providing phenological data  
286 for all stages of the life cycle of this moth in the field, is the only one of its kind to date. The model  
287 was initiated with the first adult flight in 2018 (before Julian day 200), and phenology was simulated  
288 until June 2019. For each life stage and for all observation dates, we calculated the correctness rate  
289 of presences and absences between observations and simulations.

## 2.5. Model stability

292 Given the uncertainty on the values of the parameters, we performed a model stability analysis. We  
293 focused exclusively on parameters involved in the phenology of this species, disregarding the others  
294 (e.g., fecundity or mortality rates). We considered either a range of likely values according to our  
295 knowledge (uncertainty analysis) or a standard range (e.g., degree days  $\pm$  20% and temperature  
296 threshold  $\pm$  2°C) (sensitivity analysis) when it was not possible to determine the likely range of values.  
297 The stability analysis was performed on the temperature data for Orléans in 2016 and 2017. The  
298 output variables for this analysis were the date at which diapause ended and the peak date of adult  
299 flights for each generation. When analysing the effects of each parameter, we calculated the  
300 elasticity coefficient  $\left(\frac{(y_1 - y_0)/y_0}{(x_1 - x_0)/x_0}\right)$  with  $x_0$  as the default value of the parameter,  $x_1$  as the new value  
301 of the parameter,  $y_0$  as the output variable corresponding to  $x_0$ , and  $y_1$  as the output variable  
302 corresponding to  $x_1$ . We then took the absolute value of the elasticity coefficient and calculated the  
303 maximal absolute value over the range of values of the input parameter and the output variables. It  
304 was not possible to calculate this value for all parameters tested (*Deggs* and *DUwarm*), so we also  
305 calculated the rate of variation  $(y_1 - y_0)/y_0$ , and the maximum of these absolute values.

306

1  
2  
3  
4  
5  
6  
7  
8  
9  
10  
11  
12  
13  
14  
15  
16  
17  
18  
19  
20  
21  
22  
23  
24  
25  
26  
27  
28  
29  
30  
31  
32  
33  
34  
35  
36  
37  
38  
39  
40  
41  
42  
43  
44  
45  
46  
47  
48  
49  
50  
51  
52  
53  
54  
55  
56  
57  
58  
59  
60  
61  
62  
63  
64  
65

**2.6. Model simulations in a context of climate warming**

We explored the possible effects of climate warming, by considering temperature increases of +1°C and +2°C relative to the daily minimal and maximal temperatures recorded at Orléans, Caen, Contrevoz and Basel. We compared the number of generations and calculated the percentage of days on which adult flights occurred, simulated under a climate warming scenario, for the periods of adult flight simulated for the current climate (hereafter referred to a “% similarity”). For all generations in the second year, we also compared the dates of the simulated peak numbers of adults in the current climate and in conditions of climate warming. We calculated the advance, in days, of the peaks for temperature increases of +1°C and +2°C relative to current climate conditions. Then, we calculated the mean and the maximum advances of the generations for the two climate warming scenarios.

**3. Results**

**3.1 Model validation**

Preliminary check. Each generation (from laying of the first egg to death of the last adult) took 48 days in simulations of phenology at 25°C (excluding the diapause submodel), and 51-63 days in the laboratory (according to Tabone et al. 2015). The life cycle (from laying of the first egg of one generation to laying of the first egg of the following generation) was completed within 38 days in the simulation, assuming that females began to lay eggs four days after emergence (against mean of 45 days and range of 40-50 days in the laboratory). Egg development took four days in the simulation (against 1-5 days in the laboratory). Development of the larval of groups G1, G2, and G3 took 3, 4 and 13 days, respectively, corresponding to a total of 20 days for complete larval development (against 29-33 days in the laboratory). Pupal development took 10 day in the simulation (against 9-10 days in the laboratory). The simulated life cycle at 25°C was completed slightly faster in the simulation than

331 under laboratory conditions (Tabone et al. 2015). This was mostly due to the shorter time required  
1  
2 332 for larval development in the simulations. Following activation of the diapause submodel in the  
3  
4 333 simulation, the population was unable to survive because it never met diapause conditions (the  
5  
6  
7 334 conditions for diapause induction and cold accumulation).  
8  
9

10 335 Validation 1. Correctness rates exceeded 60% at Orléans and Contrevoz, and 80% at Caen and Basel  
11  
12 336 (validation in the following year, 2010) (Table 2 and Fig. 3).  
13  
14

15 337

Site	Year of initialisation	Year of validation	% correctness
Orléans	2017	2018	66.3
Contrevoz	2017	2018	62.47
Caen	2017	2018	80
Basel	2009	2010	81.64
Basel	2009	2011	51.23
Basel	2009	2012	85.48

17 338

18  
19  
20  
21  
22  
23  
24  
25  
26  
27 339 **Table 2.** Model validation based on the presence/absence of adult stages at Orléans, Contrevoz, Caen  
28  
29 340 and Basel (initialisation on first flight in 2017 and validation in 2018 for Orléans, Contrevoz and Caen,  
30  
31  
32 341 and initialisation on the first flight in 2009 and validation in subsequent years for Basel). This table  
33  
34  
35 342 provides the correctness rate of presences/absences predictions compared to observations.  
36  
37  
38

39 343

40  
41  
42 344 However, the model simulated a third flight for Orléans at the end of 2018 that was not actually  
43  
44  
45 345 observed (Fig. 3).  
46  
47  
48  
49  
50  
51  
52  
53  
54  
55  
56  
57  
58  
59  
60  
61  
62  
63  
64  
65

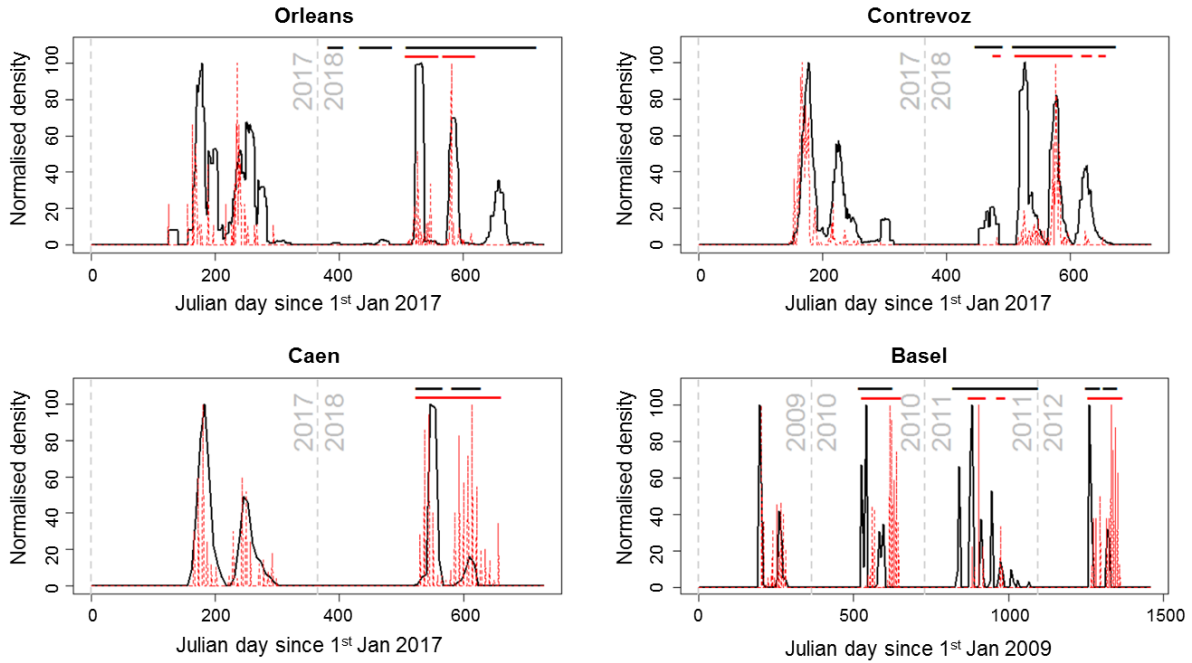
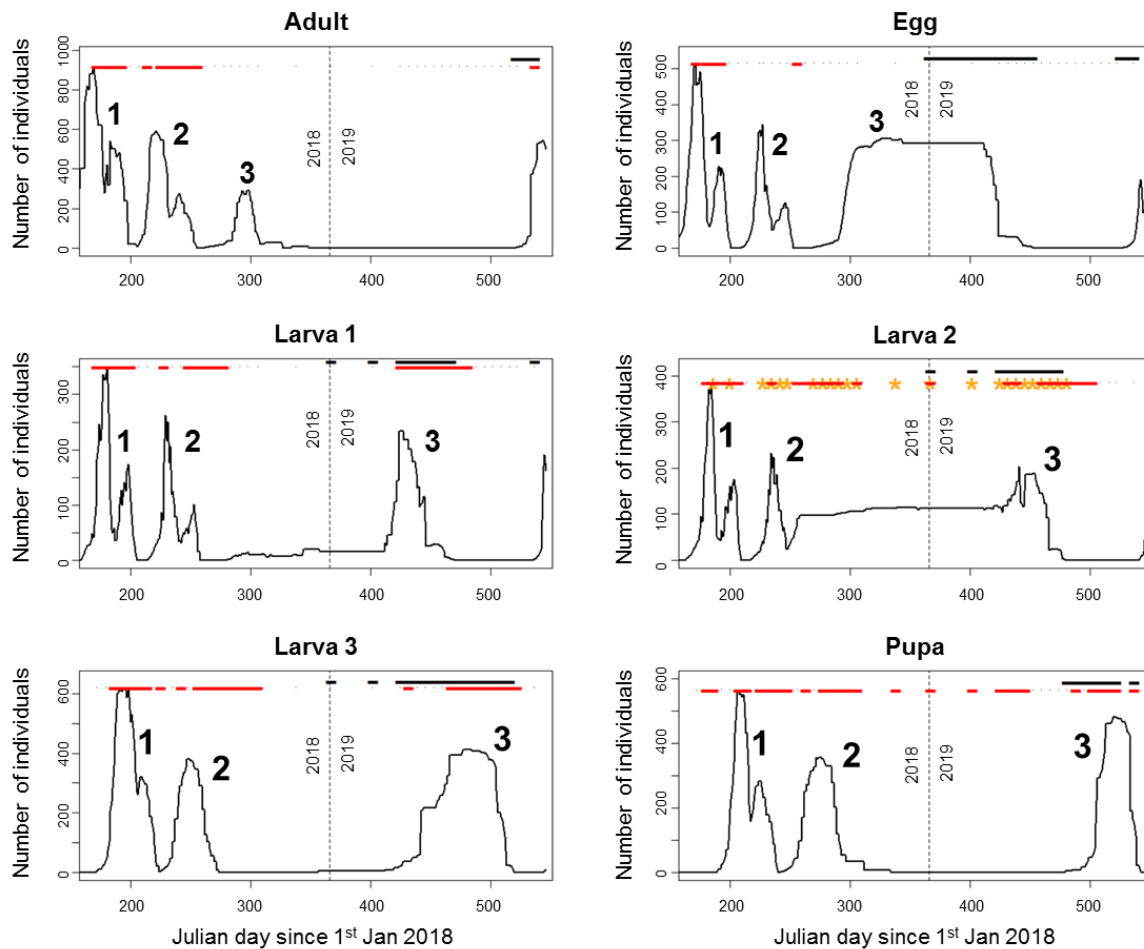


Fig. 3. Model validation at four sites. The model was initiated by the first flight of the first year and was validated on adult flights observed in subsequent years. The black curves and the red dotted curves represent the adult density (normalised by year) according to model simulations (black) and observations (red dotted). To improve clarity, the horizontal red dashed lines at the top indicate the days on which adults were observed, and the horizontal black dashed lines indicate the days on which adults were predicted to be present in model simulations for the years considered for validation purposes.

Validation 2. The model did not accumulate much error over the years. The fitting success of the model for Basel exceeded 80% (in 2010 and 2012) (Table 2). However, the simulated time window for the presence of adults was relatively large in 2011 and the model predicted earlier and later flights than were actually observed for this particular year (Fig. 3).

Validation 3. A comparison of the periods corresponding to each life stage at Orléans in 2018-2019 yielded the following results (Fig. 4; Table 3).



361  
 362 Fig. 4. Model validation on life stage data collected at Orléans in 2018-2019. Black curves represent  
 363 the abundance of the life stage based on simulations. Horizontal red dashed lines indicate the days  
 364 on which a particular life stage was observed and horizontal black dashed lines indicate the days on  
 365 which the corresponding life stage was predicted to be present in model simulations. For larva 2  
 366 (G2), asterisks indicate the days on which diapausing larvae were observed. Three generations  
 367 (numbered 1, 2 and 3) were followed. The adults of generation 1 (numbered 1) provided the eggs  
 368 numbered 1, which provided the larvae 1 numbered 1, and so on. Larva 1, 2 and 3 correspond to  
 369 larval groups G1, G2 and G3, respectively.

370  
 371 (1) The second adult flight was correctly estimated, but the simulations predicted a third adult flight  
 372 at the end of 2018 (at around day 300 – end of October 2018), which was not observed in the field  
 373 despite the presence of two pheromone traps until early November (Fig. 4). (2) Egg occurrence was

374 not correctly estimated (Table 3). (3) The occurrence of larvae of G1 was correctly estimated. The  
 1  
 2 375 model even predicted the first time of occurrence in early 2019. (4) The occurrence of G2 larvae was  
 3  
 4 376 also correctly estimated. (5) The occurrence of G3 larvae was correctly estimated, and (6) the  
 5  
 6  
 7 377 occurrence of pupae was relatively well estimated. Most correctness rates exceeded 90% (Table 3).  
 8  
 9

10 378

Life stage	Number of weeks of occurrence	Number of weeks of observation	% correctness
Adult (j>200)	8	34	94.44
Egg	5	39	61.11
Larva G1	20	39	97.09
Larva G2	23	39	95.35
Larva G3	25	39	95.35
Pupa	28	39	95.35

23 379

24  
 25  
 26 380 **Table 3.** Validation of the model of subsequent life stages at Orléans in 2018-2019. This table  
 27  
 28 381 provides, for all observation dates, the correctness rate of presences/absences predictions  
 29  
 30  
 31 382 compared to observations. For adults, this calculation was performed only for observations after  
 32  
 33 383 day 200, because the data for observations before this time point were used for model  
 34  
 35  
 36 384 initialisation.  
 37

38 385

39  
 40  
 41  
 42 386 According to these simulations (Fig. 4), the second adult flight provides individuals that  
 43  
 44 387 overwinter as G2 larvae, whereas the third adult flight provides individuals that could overwinter  
 45  
 46 388 as eggs, producing larvae in early 2019. This implies that the generations overlap, which was  
 47  
 48  
 49 389 confirmed by representations of the time windows corresponding to the development of each  
 50  
 51 390 generation (Fig. 5).  
 52  
 53  
 54  
 55  
 56  
 57  
 58  
 59  
 60  
 61  
 62  
 63  
 64  
 65

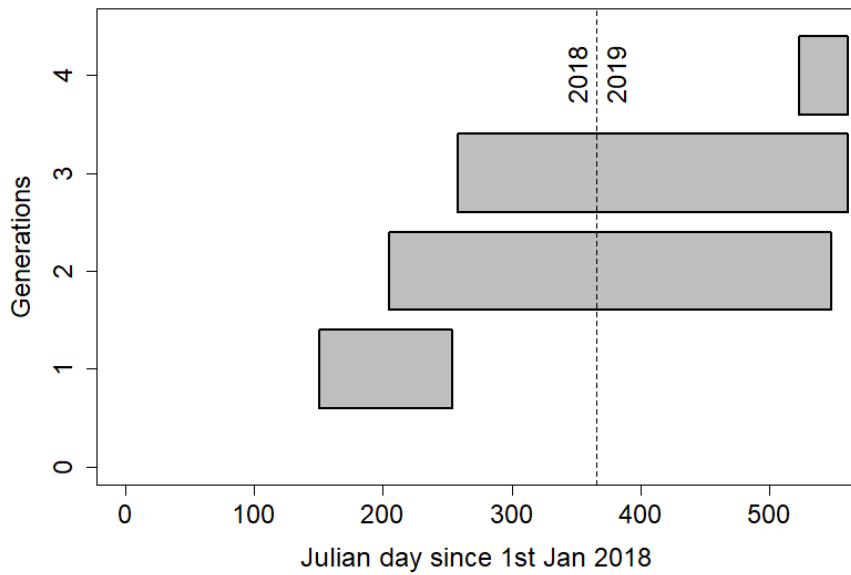


Fig. 5. Overlap between subsequent generations according to model simulations for Orléans.

Each rectangle indicates the period between the laying of the first egg and the death of the last adult.

According to the model, diapause could be induced between day 248 (September 5<sup>th</sup> 2018) and day 304 (October 31<sup>st</sup> 2018). In the field, diapausing larvae were observed from day 228 (August 16<sup>th</sup> 2018) onwards, and more than half the population (>50%) was already in diapause by day 278 (October 5<sup>th</sup> 2018). According to the model, diapause was predicted to end on day 417 (February 21<sup>st</sup> 2019), regardless of when individuals entered diapause. Observations showed that the number of diapausing larvae decreased to 0 between day 453 (March 29<sup>th</sup> 2019) and day 488 (May 5<sup>th</sup> 2019). The simulations therefore appear to predict too early an end to diapause (given that the larvae in cocoons observed in the field are effectively still in diapause).

### 3.2 Model stability

The parameter with the greatest effect was clearly *T<sub>Llarvae</sub>*, the minimal threshold above which the heat accumulation occurs in the description of larval development (Table 4, SM1). This parameter

408 should, therefore, be carefully assessed to ensure a good estimate of the species phenology.

409 Parameters relating to diapause (*DI*, *TLcold*, *DLcold* and *DUwarm*) had surprisingly little effect.

Parameter	Values tested	Elasticity	Variation
<i>DI</i>	12 and 14h	0.024	0.002
<i>TLcold</i>	0 and 4°C	0.002	0.002
<i>DLcold</i>	35 and 55 days	0.008	0.002
<i>DUwarm</i>	-2 and + 2 days (simultaneously for each value)		0.024
<i>Deggs</i>	Day 4 to 7 Day 8 to 11 Day 11 to 14		0.012
<i>L</i>	10 days (with <i>Deggs</i> = day 4 to 10) to 18 days	0.054	0.015
<i>TLeggs</i>	9 and 13°C (±2°C)	0.126	0.023
<i>DDeggs</i>	38.8 and 58.2°C days (± 20%)	0.060	0.012
<i>TLlarvae</i>	6.5 and 10.5 °C (±2°C)	<b>0.180</b>	<b>0.043</b>
<i>DDLarvae1</i>	35.6 and 53.4°C days (± 20%)	0.051	0.010
<i>DDLarvae2</i>	53.4 and 80.1°C days	0.044	0.009
<i>DDLarvae3</i>	169.0 and 253.5°C days	0.156	0.031
<i>TLpupae</i>	9.5 and 13.5°C	0.154	0.027
<i>DDpupae</i>	106.7 and 160.0°C days (± 20%)	0.126	0.025

410  
411 **Table 4.** Stability analysis. Elasticity represents the maximum of absolute values for elasticity  
412 coefficients, and variation represents the maximum of absolute values for variation rates. The  
413 numbers in bold are the highest values.

### 415 3.3 Model simulations under climate warming

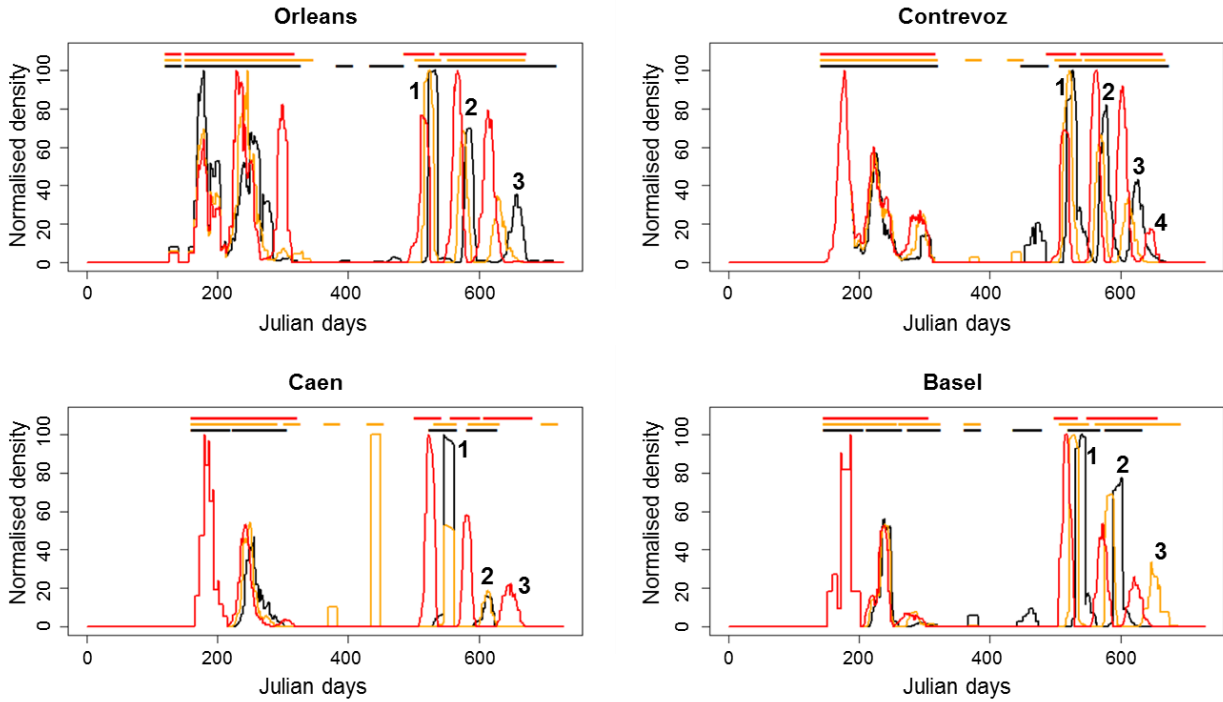
416 Insect phenology changed considerably in simulations of climate warming, but the predicted  
417 changes differed between sites. Most adult flights would be observed within the same time window  
418 as under current climatic conditions at Orléans and Contrevoz (Table 5).

Site	Scenario	% similarity	Mean advance in peak of adult occurrence (days)	Maximum advance in peak of adult occurrence (days)

<b>Orléans</b>	+1°C	90.9	15	29
<b>Orléans</b>	+2°C	91.8	28	46
<b>Contrevoz</b>	+1°C	88.0	8	15
<b>Contrevoz</b>	+2°C	88.5	16	24
<b>Caen</b>	+1°C	62.5	3	5
<b>Caen</b>	+2°C	71.9	33	33
<b>Basel</b>	+1°C	79.2	12	12
<b>Basel</b>	+2°C	75.1	24	25

**Table 5.** Changes in adult flight patterns in the context of different climate warming scenarios (+1°C or +2°C) relative to simulations of adult flights based on temperatures in 2017-2018 for Orléans, Contrevoz and Caen, and 2011-2012 for Basel. The mean and maximum numbers of days of advance in the peak of adults' occurrence in conditions of climate warming are compared with the adult flights in current conditions, in 2018.

The predicted changes were largest for Caen and Basel, at which flight similarity was lower than at other sites (Table 5). On average, at all four sites, the peak of adult flights would generally occur earlier for an increase of +1°C (mean of 9.5 days) and still more for an increase of +2°C (mean of 25 days). The number of generations could reach three at Orléans, Caen and Basel, and even four at Contrevoz for an increase in temperature of 2°C (Fig. 6).



431  
432 Fig. 6 Adult flight periods under scenarios of climate warming. Black curves represent the density of  
433 adults present under observed current climatic conditions (2017-2018 for Orléans, Contrevoz and  
434 Caen; and 2011-2012 for Basel), orange curves represent adult density in a scenario involving a +1°C  
435 increase in temperature, and red curves represent adult density in a scenario including a +2°C  
436 increase in temperature. The adult density was normalised by scenario and year. Generations are  
437 numbered 1, 2, 3 and 4 for the scenario with a temperature increase of +2°C. For the sake of clarity,  
438 horizontal black, orange and red dashed lines indicate the days on which adults are predicted to be  
439 present in model simulations for the three scenarios (baseline conditions, +1°C and +2°C,  
440 respectively).

441  
442 **4. Discussion**

443 **4.1 What do the model simulations and discrepancies tell us?**

444 This study provides the first version of a phenology model for the invasive box tree moth. The model  
445 provided rough estimates of the time window for each life stage and did not accumulate much error

1  
2  
3  
4  
5  
6  
7  
8  
9  
10  
11  
12  
13  
14  
15  
16  
17  
18  
19  
20  
21  
22  
23  
24  
25  
26  
27  
28  
29  
30  
31  
32  
33  
34  
35  
36  
37  
38  
39  
40  
41  
42  
43  
44  
45  
46  
47  
48  
49  
50  
51  
52  
53  
54  
55  
56  
57  
58  
59  
60  
61  
62  
63  
64  
65

446 over the years. It predicted two or three generations per year, which is consistent with the available  
447 observations. This model revealed a complex dynamics of invasive populations of box tree moth: 1)  
448 several generations overlap, making it difficult to distinguish between flight periods, and 2) the insect  
449 may potentially overwinter not only as a larva, but also at other life stages, and 3) climate warming  
450 may enhance this phenomenon in the future. However, these model simulation outputs require  
451 confirmation in the field.

452 In cases of discrepancy between simulations and observations, it was not possible to provide a clear  
453 explanation for the differences, which may result from an error in the model simulations or from a  
454 bias in the observations. Two main discrepancies require further investigation: 1) the presence of  
455 eggs and young larvae in the winter, and 2) diapause duration.

456 1) The simulations suggested that eggs might be present in the winter, whereas they are not  
457 observed in the field during this period. Nevertheless, it is very difficult to detect eggs, which are tiny  
458 and transparent, and generally located on the underside of box tree leaves. The model suggested  
459 that eggs could overwinter and provide first instar larvae (L1) in the spring, which was an unexpected  
460 result. It will therefore be important to address the following question: are eggs (and young larvae)  
461 able to survive the cold temperatures in winter or to survive to a very low development during this  
462 cold period? The collection of more field data will be required to answer this question. Meanwhile,  
463 for exploration of the effects of cold temperatures, we modified the model to include an additional  
464 mortality parameter related to low temperatures during the winter (data not shown). However, the  
465 modified model was unable to simulate the occurrence of young larvae in early spring, as observed in  
466 the field. The presence of young larvae in early spring is consistent with the presence and survival of  
467 eggs during the winter, which could then develop into L1 during the spring. Furthermore, our  
468 simulations suggest that, with climate warming, we will probably observe more eggs and young  
469 larvae in winter (data not shown). This issue of the possible survival of both eggs and young larvae in

1  
2 470 winter is, therefore, extremely important in the context of climate warming. Laboratory experiments  
3  
4 471 could be performed to address this question.

5 472 2) The time window for diapause duration was underestimated by the model in validation 3.  
6  
7 473 However, the larvae observed in cocoons in the field may not necessarily actually be in diapause (i.e.,  
8  
9 474 interrupted development). If they build their cocoon before entering diapause and remain within the  
10  
11 475 cocoon for a short period after the end of diapause, this would bias the observation dataset relating  
12  
13 476 to diapause in the field. Accurate validation of the diapause period on the basis of field data is  
14  
15 477 complex. Another issue concerning diapause emerged from the preliminary check (at a constant  
16  
17 478 temperature of 25°C). In simulations without the diapause submodel, the development rates  
18  
19 479 obtained for each life stage were very similar to those observed in laboratory conditions. Indeed, no  
20  
21 480 diapause is observed in the constant conditions of the laboratory (temperature 25°C, photoperiod  
22  
23 481 16L:8D). The photoperiod is constant and longer than the threshold period of 13 h, preventing the  
24  
25 482 induction of diapause. When we simulated phenology at 25°C with the diapause submodel, the  
26  
27 483 simulations showed a population crash in the winter (data not shown). The model should be refined  
28  
29 484 further, to determine whether larvae fail to enter diapause under some temperature conditions.  
30  
31  
32  
33  
34  
35

36 485 According to our findings, the box tree moth can have more than two generations in Europe, and  
37  
38 486 may even produce four generations in conditions of climate warming with an increase in  
39  
40 487 temperature of 2°C, at the sites studied. Climate warming may therefore accelerate the already very  
41  
42 488 rapid spread of this invasive species. In addition, we set female fecundity to a very low value ( $F = 2$ )  
43  
44 489 to avoid a population explosion. Population growth is a key factor in the rapid spread of this pest and  
45  
46 490 high population abundance will clearly have a major effect on box trees, some of which may be  
47  
48 491 heavily, or even completely defoliated, leading to their death (Kenis et al. 2013, Mitchell et al. 2018).  
49  
50 492 At this point, low resource availability might lead to a decrease in the abundance of box tree moths.  
51  
52  
53  
54  
55

#### 56 493 ***4.2 Limitations of the model***

57  
58  
59  
60  
61  
62  
63  
64  
65

1  
2  
3  
4  
5  
6  
7  
8  
9  
10  
11  
12  
13  
14  
15  
16  
17  
18  
19  
20  
21  
22  
23  
24  
25  
26  
27  
28  
29  
30  
31  
32  
33  
34  
35  
36  
37  
38  
39  
40  
41  
42  
43  
44  
45  
46  
47  
48  
49  
50  
51  
52  
53  
54  
55  
56  
57  
58  
59  
60  
61  
62  
63  
64  
65

494 The current model is not spatially explicit. However, it could be used to explore the spatial impact of  
495 different temperature conditions (and climate, in the long term) on temporal dynamics. It could be  
496 applied to sites in different countries, provided that the box tree moth populations at these sites  
497 originate from the same source population as the population studied in Switzerland (development  
498 thresholds from Nacambo et al. 2014), and thus present similar thermal development thresholds. In  
499 Europe, the invasion pathway followed by this moth appears to be complex, probably involving  
500 several genetic processes (Bras et al. 2019). Nevertheless, an eastern Chinese origin has been  
501 proposed for all invasive populations across Europe and Asia Minor studied to date (Bras et al. 2019),  
502 suggesting that all these populations may have similar development thresholds, making it possible to  
503 use our model at a larger scale. In addition, we did not consider an upper temperature threshold for  
504 development. If the model is applied to a site in an area warmer than those studied here (e.g.  
505 southern Europe), where temperatures frequently exceed 35°C, an upper threshold should be  
506 considered. Without such a threshold, the model may be subject to limitations at high temperatures,  
507 resulting in a possible overestimation of development rates.

508 In this study, we considered the maximum and minimum daily temperatures recorded by weather  
509 stations. We assumed these temperatures to be representative of the temperatures actually  
510 experienced by the box tree moth individuals. However, microclimate conditions are known to  
511 display considerable spatial variation and to have a large impact on insects (Kearney and Porter 2009,  
512 Pincebourde et al. 2016). Eggs and larvae are generally found on box tree leaves. Only diapausing  
513 larvae and pupae are likely to be protected, within their cocoon, wrapped in a leaf. The outputs of  
514 simulations could, therefore, be refined by considering temperature at a local scale rather than the  
515 temperatures recorded by weather stations.

#### 516 ***4.3 Usefulness of the model in terms of pest management***

517 Box trees do not have a particularly high economic value, but the decline of ornamental box trees  
518 and natural box tree stands would nevertheless have a major ecological, cultural and social impact

1  
2  
3  
4  
5  
6  
7  
8  
9  
10  
11  
12  
13  
14  
15  
16  
17  
18  
19  
20  
21  
22  
23  
24  
25  
26  
27  
28  
29  
30  
31  
32  
33  
34  
35  
36  
37  
38  
39  
40  
41  
42  
43  
44  
45  
46  
47  
48  
49  
50  
51  
52  
53  
54  
55  
56  
57  
58  
59  
60  
61  
62  
63  
64  
65

519 (Mitchell et al. 2018). The development of effective control measures against box tree moth has  
520 therefore received considerable attention. Our model provides an appropriate framework for  
521 improving the management of this multivoltine species in the near future. Indeed, several  
522 environmentally friendly control measures could be applied, targeting particular life stages of the  
523 moth.

524 Hereafter, we shortly review three of them. 1) Pheromone traps capture adult males, and can  
525 therefore be installed during adult flight periods, which may be quite long. If the traps are in place  
526 unnecessarily for several months, the pheromone baits should be regularly replaced, to ensure that  
527 the traps remain effective. Precise assessments of the time window for adult flights with the model  
528 presented here would be useful for optimising this method, ensuring that traps were installed only  
529 when necessary (either for population monitoring or for a tentative of mass trapping). The catching  
530 of adult females would also be of great interest, and a female-targeting lure should become available  
531 in the near future (Molnár et al. 2019). 2) *Bacillus thuringiensis* sprays can be used against young  
532 larvae (Göttig 2017). If applied at the wrong time (i.e., too early, on eggs, or too late, on older larval  
533 instars) this method may not efficiently protect ornamental box trees against feeding larvae. For this  
534 control method, our model can estimate the timing of larval emergence and provide an indication of  
535 the time window during which first larval instars are present, making it possible to optimise  
536 treatment efficacy. 3) Classical biological control involves releasing a specific natural enemy targeting  
537 the egg stage, to control the population before the larvae have an opportunity to feed on and  
538 defoliate box trees (e.g. using *Trichogramma* sp. as biological agents; Göttig 2017, Enriquez et al.  
539 2015). The model can predict the time window for egg occurrence, corresponding to the period in  
540 which the parasitoids should be released.

541 Identifying the appropriate time window for each control method would increase control efficacy.  
542 Furthermore, in newly invaded regions, such as North America, where this insect was first detected  
543 in August 2018 (Frank 2019), our model is of major potential interest to stakeholders to facilitate the

1  
2 544 implementation of efficient management strategies at early stages of box tree moth invasion. This  
3  
4 545 model could also feed into platforms, such as the Degree-Days, Risk, and Phenological event mapping  
5  
6 546 (DDRP) platform (Barker et al. 2020).  
7

#### 8 547 **4.4 Key message**

9  
10 548 The model developed here goes far beyond a simple degree-day model, as it accounts for  
11  
12 549 photoperiod, diapause processes, and population growth parameters. Models of this type appear to  
13  
14 550 be particularly useful for identifying knowledge gaps and disentangling overlaps between the life  
15  
16 551 stages of invasive species (Nielsen et al. 2016). This model is also a potentially useful tool for  
17  
18 552 assessing potential population growth (including the number of generations) in invaded areas and,  
19  
20 553 thus, for fine-tuning estimates of the risk of rapid invasions due to the potential growth rate of the  
21  
22 554 pest. In addition, in the context of climate warming, population phenology may become more erratic,  
23  
24 555 and models of this type can provide an important cornerstone in efforts to improve control methods  
25  
26  
27  
28  
29 556 targeting specific life stages.  
30  
31  
32  
33  
34  
35  
36  
37  
38  
39  
40  
41  
42  
43  
44  
45  
46  
47  
48  
49  
50  
51  
52  
53  
54  
55  
56  
57  
58  
59  
60  
61  
62  
63  
64  
65

557 **References**

- 1  
2  
3 558 Barker, B.S., Coop, L., Wepprich, T., Grevstad, F., Cook, G., 2020. DDRP: real-time phenology and  
4 climatic suitability modeling of invasive insects. BioRxiv, doi:10.1101/2020.05.18.102681  
5 559  
6  
7 560 Bonhomme, R., 2000. Bases and limits to using 'degree.day' units. Eur. J. Agron., 13, 1–10.  
8  
9  
10 561 Boukal, D. S., and Berec, L., 2002. Single-species models of the Allee effect: extinction boundaries, sex  
11 562 ratios and mate encounters. J. Theor. Biol., 218(3), 375-394.  
12  
13 563 <https://doi.org/10.1006/jtbi.2002.3084>  
14  
15  
16 564 Bras, A., (2018). Identification des facteurs sous-tendant l'invasion fulgurante d'un insecte asiatique  
17 565 en Europe, la pyrale du buis: approche génétique et biologique. PhD thesis, Université d'Orléans  
18 (France), pp. 243.  
19 566  
20  
21 567 Bras, A., Avtzis, D.N., Kenis, M., Li, H., Véték, G., Bernard, A., Courtin, C., Rousselet, J., Roques, A.,  
22 568 Auger-Rozenberg, M-A., 2019. A complex invasion story underlines the fast spread of the invasive  
23 box tree moth (*Cydalima perspectalis*) across Europe. J. Pest. Sci., 92, 1187-1202.  
24 569  
25  
26 570 Damos, P., Savopoulou-Soultani, M., 2012. Temperature-driven models for insect development and  
27 571 vital thermal requirements. Psyche, Article ID 123405, doi:10.1155/2012/123405  
28  
29  
30 572 Dehnen-Schmutz, K., Holdenrieder, O., Jeger, M.J., Pautasso, M., 2010. Structural change in the  
31 573 international horticultural industry: some implications for plant health. Sci. Hortic-Amsterdam,  
32 574 125, 1-15.  
33  
34  
35 575 Dlugosch, K.M., Parker, I.M., 2008. Founding events in species invasions: genetic variation, adaptive  
36 576 evolution, and the role of multiple introductions. Mol. Ecol., 17, 431–449.  
37  
38  
39 577 Enriquez, T., Giorgi, C., Venard, M., Colombel, E., Gaglio, F., Buradino, M., Martin, J-C., Tabone, E.,  
40 578 2015. Des souches de trichogramme contre la pyrale du buis. Phytoma, 685, 21-24.  
41  
42  
43 579 Fahrner, S., Aukema, B.H., 2018. Correlates of spread rates for introduced insects. Global. Ecol.  
44 580 Biogeogr., 27, 734-743.  
45  
46  
47 581 Frank, S., 2019. Watch for potential new boxwood pest. The Purdue Landscape Report, 19(2),1–4.  
48 582  
49  
50 583 Gninenko, Yu.I., Shiryayeva, N.V., Shurov, V.I., 2014. The box tree moth - a new invasive pest in the  
51 584 Caucasian Forests. Plant Health - Research and Practice, 1, 32–39.  
52  
53  
54 585 Göttig, S.G., 2017. Development of eco-friendly methods for monitoring and regulating the box tree  
55 586 pyralid, *Cydalima perspectalis* (Lepidoptera: Crambidae), an invasive pest in ornamentals. PhD  
56  
57  
58  
59  
60  
61  
62  
63  
64  
65

- 586 thesis, Technische Universität Darmstadt (Germany), pp. 130.  
1  
2 587 <http://tuprints.ulb.tu-darmstadt.de/6855/1/Dissertation%20Stefanie%20G%C3%B6ttig.pdf>  
3  
4 588 Haond, M., Morel-Journel, T., Lombaert, E., Vercken, E., Mailleret, L., Roques, L., 2018. When higher  
5 carrying capacities lead to faster propagation. bioRxiv, 307322; [https://hal.archives-](https://hal.archives-ouvertes.fr/hal-01877823/document)  
6 589 [ouvertes.fr/hal-01877823/document](https://hal.archives-ouvertes.fr/hal-01877823/document)  
7  
8 590  
9  
10 591 Kearney, M., Porter, W., 2009. Mechanistic niche modelling: combining physiological and spatial data  
11 to predict species' ranges. Ecol. Lett., 12, 334-350.  
12  
13  
14 593 Kenis, M., Nacambo, S., Leuthardt, F.L.G., Di Dominico, F., Haye, T., 2013. The box tree moth:  
15 *Cydalima perspectalis*, in Europe: horticultural pest or environmental disaster? Aliens, 33, 38-41.  
16 594  
17  
18 595 Klein Tank, A.M.G. and Coauthors, 2002. Daily dataset of 20th-century surface air temperature and  
19 precipitation series for the European Climate Assessment. Int. J. of Climatol., 22, 1441-1453.  
20 596  
21  
22  
23 597 Lepilleur, T., Brancaccio, L., Ben Soussan, T., Baby, P., Aveline, S., Duval, C., 2017. Efficacité des  
24 trichogrammes contre la pyrale du buis. Phytoma, 705, 20-25 [http://www.phytoma-](http://www.phytoma-ldv.com/revue-1802-PHYTOMA-705)  
25 598 [ldv.com/revue-1802-PHYTOMA-705](http://www.phytoma-ldv.com/revue-1802-PHYTOMA-705)  
26 599  
27  
28  
29 600 Maruyama, T., Shinkaji, N., 1991. The life-cycle of the box-tree pyralid, *Glyphodes perspectalis*  
30 (Walker) (Lepidoptera: Pyralidae). II. Developmental characteristic of larvae. Jpn J Appl Entomol  
31 601 Zool, 35, 221-230.  
32  
33  
34  
35 603 Matošević, D., Lukić, I., Bras, A., Lacković, N., Pernek, M., 2017. Spatial distribution, genetic diversity  
36 and food choice of box tree moth (*Cydalima perspectalis*) in Croatia. SEEFOR, 8, 41–46.  
37 604  
38 605 <https://doi.org/10.15177/seeфор.17-06>  
39  
40  
41 606 Mitchell, R., Chitanava, S., Dbar, R., Kramarets, V., Lehtijärvi, A., Matchutadze, I., Mamadashvili, G.,  
42 Matsiakh, I., Nacambo, S., Papazova-Anakieva, I.P., Sathyapala, S., Tuniyev, B., Véték, G.,  
43 607 Zukhbaia, M., Kenis, M. 2018. Identifying the ecological and social consequences of a decline in  
44 608 *Buxus* forests in Europe and the Caucasus. Biol. Invasions, 20, 3605-3620.  
45  
46 609  
47  
48  
49 610 Molnár, B.P., Kárpáti, Z., Nagy, A., Szarukán, I., Csabai, J., Koczor, S., Tóth, M., 2019. Development of  
50 611 a female-targeted lure for the box tree moth *Cydalima perspectalis* (Lepidoptera: Crambidae): a  
51 preliminary report. J. Chem. Ecol., 45, 657-666.  
52 612  
53  
54  
55 613 Nacambo, S., Leuthardt, F.L.G., Wan, H., Li, H., Haye, T., Baur, B., Weiss, R.M., Kenis, M., 2014.  
56 614 Development characteristics of the box-tree moth *Cydalima perspectalis* and its potential  
57 distribution in Europe. J. Appl. Entomol., 138, 14-26.  
58 615  
59  
60  
61  
62  
63  
64  
65

616 Nielsen, A.L., Chen, S., Fleischer, S.J., 2016. Coupling developmental physiology, photoperiod, and  
1 617 temperature to model phenology and dynamics of invasive heteropteran *Halyomorpha halys*.  
2  
3 618 Front. Physiol., 7, 165. <https://doi.org/10.3389/fphys.2016.00165>  
4  
5  
6 619 Ochocki, B.M., Miller, T.E.X., 2017. Rapid evolution of dispersal ability makes biological invasions  
7  
8 620 faster and more variable. Nat. Commun., 8, 14315. <https://doi.org/10.1038/ncomms14315>  
9  
10 621 Pincebourde, S., Murdock, C. C., Vickers, M., Sears, M. W., 2016. Fine-scale microclimatic variation  
11  
12 622 can shape the responses of organisms to global change in both natural and urban environments.  
13  
14 623 Integr. Comp. Biol., 56, 45-61. <https://doi:10.1093/icb/icw016>  
15  
16 624 Pineau, P., Lorme, P., Bernard, A., Bras, A., Poitou, L., Rousselet, J., Robinet, C., 2020. Records of the  
17  
18 625 box tree moth, *Cydalima perspectalis*, phenology in Orleans and Contrevoz (France).  
19  
20 626 <https://doi.org/10.5281/zenodo.3719293>  
21  
22 627 Poitou, L., 2018. Rôles de la température et de la photopériode sur la levée de la diapause hivernales  
23  
24 628 chez une espèce dont l'invasion est fulgurante en Europe, la pyrale du buis, *Cydalima perspectalis*  
25  
26 629 (Lepidoptera, Crambidae). Master thesis, Université de Bordeaux (France), pp. 23.  
27  
28 630 Pollard, C.P., Griffin, C.T., de Andrade Moral, R., Duffy, C., Chuche, J., Gaffney, M.T., Fealy, R.M.,  
29  
30 631 Fealy, R., 2020. phenModel: A temperature-dependent phenology/voltinism model for a  
31  
32 632 herbivorous insect incorporating facultative diapause and budburst. Ecol. Model., 416.  
33  
34 633 <https://doi.org/10.1016/j.ecolmodel.2019.108910>  
35  
36 634 Rebaudo, F., Rabhi, V.-B., 2018. Modeling temperature-dependent development rate and phenology  
37  
38 635 in insects: review of major developments, challenges, and future directions. Entomol. Exp. Appl.,  
39  
40 636 166, 607–617.  
41  
42 637 Robinet, C., Liebhold, A., Gray, D., 2007. Variation in developmental time affects mating success and  
43  
44 638 Allee effects. Oikos, 116: 12271.  
45  
46 639 Robinet, C., Suppo, C., Darrouzet, E., 2017. Rapid spread of the invasive yellow-legged hornet in  
47  
48 640 France: the role of human-mediated dispersal and the effects of control measures. J. Appl. Ecol.,  
49  
50 641 54, 205-215.  
51  
52 642 Robinet, C., Suppo, C., 2020. R script to simulate the phenology of the box tree moth, *Cydalima*  
53  
54 643 *perspectalis*. <https://doi.org/10.5281/zenodo.3719273>  
55  
56  
57 644 R Core Team (2019) R: A language and environment for statistical computing. R Foundation for  
58  
59 645 Statistical Computing, Vienna, Austria. URL <https://www.R-project.org/>.  
60  
61  
62  
63  
64  
65

- 646 Roques, A., 2010. Taxonomy, time and geographic patterns, in: Roques, A. et al. (Eds), Alien  
1 647 terrestrial arthropods of Europe. *BioRisk*, 4, 11-26.  
2  
3
- 4 648 Roques, A., Auger-Rozenberg, M-A., Blackburn, T.M., Garnas, J., Pyšek, P., Rabitsch, W., Richardson,  
5  
6 649 D.M., Wingfield, M.J., Liebold, A.M., Ducan, R.P., 2016. Temporal and interspecific variation in  
7  
8 650 rates of spread for insect species invading Europe during the last 200 years. *Biol. Invasions*, 18,  
9  
10 651 907-920.  
11
- 12 652 Seebens, H., Blackburn, T.M., Dyer, E.E., Genovesi, P., Hulme, P.E., Jeschke, J.M., Pagad, S., Pyšek, P.,  
13  
14 653 Winter, M., Arianoutsou, M. et al., 2017. No saturation in the accumulation of alien species  
15  
16 654 worldwide. *Nat. Commun.* , 8, 14435.  
17
- 18 655 Shigesada, N., Kawasaki, K., 1997. *Biological Invasions: theory and practice*. Oxford University Press,  
19  
20 656 pp. 205.  
21
- 22 657 SoDa team (2019) Solar Energy Services for Professionals. Available at: <http://www.soda-pro.com>.  
23  
24 658 Accessed 14 January 2019.  
25
- 26 659 Tabone, E., Enriquez, T., Giorgi, C., Venard, M., Colombel, E., Gaglio, F., Buradino, M., Martin, J-C.,  
27  
28 660 2015. Mieux connaître la pyrale du buis *Cydalima perspectalis*. *Phytoma*, 685, 18-20.  
29
- 30  
31 661 Taylor, C.M., Hastings, A., 2005. Allee effects in biological invasions. *Ecol. Lett.*, 8, 895-908.  
32
- 33 662 Wan, H., Haye, T., Kenis, M., Nacambo, S., Xu, H., Zhang, F., Li, H., 2014. Biology and natural enemies  
34  
35 663 of *Cydalima perspectalis* in Asia: is there biological control potential in Europe? *J. Appl. Entomol.*,  
36  
37 664 138, 715-722. doi:10.1111/jen.12132  
38
- 39 665 Xiao, H-J., Xin, H-Q., Zhu, X-F., Xue, F-S., 2011. Photoperiod and temperature of diapause induction in  
40  
41 666 *Diaphania perspectalis* (Lepidoptera: Pyralidae). *Chinese J. Appl. Entomol.*, 48(1), 116–120.  
42
- 43 667 Zalom, F.G., Goodell, P.B., Wilson, L.T., Barnett, W.W., Bentley, W.J., 1983. Degree-days: the  
44  
45 668 calculation and use of heat units in pest management. University of California Division of  
46  
47 669 Agriculture and Natural Resources, leaflet 21373, pp. 10.  
48  
49  
50  
51  
52  
53  
54  
55  
56  
57  
58  
59  
60  
61  
62  
63  
64  
65

670 **Acknowledgements**

1  
2  
3 671 We thank Laura Poitou and Mathieu Laparie (INRAE URZF) for their work on the box tree moth  
4  
5 672 diapause and for providing data to feed the model, Jérôme Rousselet (INRAE URZF) for supervising  
6  
7 673 field observations, Patrick Pineau and Philippe Lorme (INRAE URZF) for collecting phenology data in  
8  
9  
10 674 Orléans, Alexis Bernard (INRAE URZF) for installing and retrieving pheromone traps and solving  
11  
12 675 technical field problems, Elisabeth Tabone, Jean-Claude Martin and Maurane Buradino (INRAE UEFM)  
13  
14  
15 676 for providing useful information about the biology of this species, Eric Hell (CRPF) and Olivier Baubet  
16  
17 677 (DSF) for helping us to find an appropriate site at Contrevoz and the townhall of Contrevoz for  
18  
19  
20 678 hosting a pheromone trap, Benoit Coiffiers (FREDON) for providing phenology data in Caen, and Marc  
21  
22 679 Kenis (CABI) for providing data in Switzerland. We sincerely thank Marie-Anne Auger-Rozenberg for  
23  
24 680 the coordination of the INCA project in which this study was conducted. We thank INRAE Agroclim  
25  
26  
27 681 and Météo-France for providing daily minimum and maximum temperatures for the French sites.  
28  
29

30 682

33 683 **Funding**

34  
35  
36 684 We acknowledge support for this work from the INCA project (Invasion fulgurante de la pyrale du  
37  
38 685 buis *Cydalima perspectalis* en Région Centre Val de Loire) funded by French region *Région Centre Val*  
39  
40  
41 686 *de Loire*.  
42  
43  
44  
45  
46  
47  
48  
49  
50  
51  
52  
53  
54  
55  
56  
57  
58  
59  
60  
61  
62  
63  
64  
65